Formation Tracking and Obstacle Avoidance for Multiple Quadrotors With Static and Dynamic Obstacles

Juntong Qi, Jinjin Guo, Mingming Wang, Chong Wu, *Member, IEEE*, and Zhenwei Ma

***Abstract*—This letter proposes a novel distributed cooperative control algorithm to address the problem of collision avoidance and obstacle avoidance for multiple quadrotors during the formation tracking process. The proposed algorithm couples collision avoidance and obstacle avoidance schemes into the control layer. To avoid collisions between quadrotors in time, a repulsion function based on Hooke's law with damping is proposed, which fully considers the relative position and relative velocity between quadrotors. In addition, based on the obstacle avoidance behavior of pigeons, a split-merge strategy is designed for multiple quadrotors to avoid static and dynamic obstacles. The split-merge strategy is driven by the relative position between the quadrotors and the obstacles, and it can calculate the optimal velocity to keep the quadrotors away from obstacles in the field of view. Several simulations and outdoor experiments for multiple quadrotors are presented to verify the effectiveness of the theoretical results.**

***Index Terms*—Aerial systems: applications, multi-robot systems, obstacle avoidance, collision avoidance, formation tracking.**

I. Introduction

A. Background and Motivation

Recently, quadrotors have been widely used in various military and civilian fields by virtue of their strong flexibility [1], [2]. Compared with a single quadrotor, multiple quadrotors can perform surveillance, reconnaissance and target attack simultaneously, which greatly improves the mission success rate and execution efficiency [3], [4]. One of the key problems in the cooperative control of multiple quadrotors is how to ensure that quadrotors can form the desired formation. It should be noted that in many practical applications [1], [3], [4], dynamic formation is better than fixed formation for multiple quadrotors to adapt to environmental changes. Furthermore, obstacle avoidance and collision avoidance are also guarantees for multiple quadrotors to perform tasks in complex environments [5].

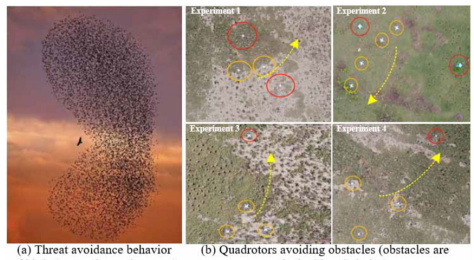

(a) Threat avoidance behavior of birds (separation and merger) (b) Quadrotors avoiding obstacles (obstacles are marked with red circles)

Fig. 1. Obstacle avoidance in nature and outdoor experiments.

In a complex environment, the traditional centralized control method cannot deal well with the impact of environmental changes [6]. It is necessary for multiple quadrotors to quickly make decisions in response to dynamic changes in the environment by interacting with their neighbors. Observations of social animals show that they can quickly form orderly formations in a complex environment, which can not only effectively avoid external threats but also ensure that they do not collide with each other. Research on the characteristics of biological swarms is conducive to designing the autonomous control of multiple quadrotors. For example, pigeon flocks have the characteristics of self-organization and self-coordination when dealing with threats or avoiding obstacles (Fig. 1(a)). If the pigeon flight mechanism is mapped to the autonomous control of multiple quadrotors, quadrotors can work in a complex environment with the ability to self-organize. The motivation of this letter is to design formation control with collision avoidance between quadrotors and obstacle avoidance for multiple quadrotors.

B. Related Work

The formation control of quadrotors has attracted many scholars and the classic formation control approach falls into three categories, leader-follower [7], behavior-based approach [8] and virtual structure approach [9]. Over the past ten years, a consensus protocol-based approach has been proposed to achieve formation control of multiple quadrotors [10], [11] and the above three classic formation control approaches have been proven to be special cases of the consensus-based ones [12]. In [13], a distributed robust controller based on consistency protocol was

Manuscript received August 9, 2021; accepted December 23, 2021. Date of publication January 6, 2022; date of current version January 19, 2022. This letter was recommended for publication by Associate Editor B. C. Arrue and Editor P. Pounds upon evaluation of the reviewers' comments. This work was supported by the National Natural Science Foundation of China under Grant 61873182. *(Juntong Qi and Jinjin Guo are co-first authors.) (Corresponding author: Mingming Wang.)*

Juntong Qi, Jinjin Guo, Mingming Wang, and Zhenwei Ma are with the School of Electrical and Information Engineering, Tianjin University, Tianjin 300072, China (e-mail: qijt@tju.edu.cn; guojinj@tju.edu.cn; wangmm19@tju.edu.cn; mzw_tju@qq.com).

Chong Wu is with the EFY Intelligent Control (Tianjin) Technology Company Ltd., Tianjin 300450, China (e-mail: wuchong18@126.com).

This letter has supplementary downloadable material available at https://doi.org/10.1109/LRA.2022.3140830, provided by the authors.

Digital Object Identifier 10.1109/LRA.2022.3140830

designed for multiple quadrotors to achieve stable formation, but it was not verified for dynamic formation. In [14], [15], a formation tracking protocol was presented for multiple second-order nonlinear systems to achieve fixed formation and dynamic formation, however, collision avoidance between quadrotors was not considered. To avoid collision in formation tracking for agents, the artificial potential field (APF) was introduced and a distributed formation tracking algorithm was proposed for a second-order linear system [16]. However, a quadrotor is a multi-input and multi-output nonlinear system involving translational and rotational dynamics. The second-order model is slightly inaccurate when dealing with the position and attitude of the quadrotor. Besides, in the collision avoidance between agents, only the relative position is considered, not the relative velocity. It is obviously unable to effectively avoid the collision between quadrotors.

Furthermore, multiple agents need to avoid static or dynamic obstacles to ensure safe flight in the environment. Several classical obstacle avoidance strategies have been developed, including the APF [17], [18] and MPC [19], [20]. In recent years, an increasing number of researchers have been interested in the combination of biological swarms and multiple quadrotors. In [6], [21], and [22], biological collective behavior was applied to the quadrotor system to realize autonomous decision-making through information interaction with neighboring quadrotors. However, the above results lack the verification of avoiding dynamic obstacles. Pigeons rely on visual perception to obtain the relative position with obstacles and fly toward the maximum gap between obstacles to complete obstacle avoidance. In [23], a modeling framework for pigeon obstacle avoidance was designed by analyzing the data of pigeons crossing a forest. In [24], the obstacle avoidance behavior of pigeons was preliminarily verified for multiple quadrotors in a static obstacle environment. However, there are few studies in the field of dynamic obstacle avoidance. Biological collective behavior provides us with solutions in this field.

C. Contributions

In this letter, a distributed cooperative control algorithm based on consensus theory and the obstacle avoidance behavior of pigeons is proposed for multiple quadrotors in obstacles environment. Compared with the aforementioned results on multi-agent system formation control, the contributions of this paper are threefold. First, this letter coupled the collision avoidance and the dynamic obstacle avoidance with the control layer. Second, considering the relative position and velocity between quadrotors in formation tracking, a repulsion function is designed based on Hooke's law with damping to ensure collision avoidance between quadrotors. Then, based on the pigeons' obstacle avoidance mechanism, a split-merge strategy is designed to avoid static and dynamic obstacles in the field of vision of quadrotors. Compared with [23], the heading angles of quadrotors do not need to be considered, and the steering velocity of quadrotors can be adjusted in real-time to ensure the safety and smoothness of the position trajectory. The third contribution is to build a multiple quadrotors experimental platform, and the results of several experiments show the effectiveness of the proposed method for different scenarios with static and dynamic obstacles. Outdoor experiments are shown in Fig. 1(b).

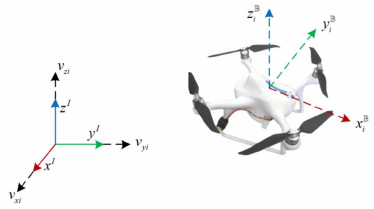

Fig. 2. Diagram of quadrotor coordinate system.

II. Problem Statement

A simple diagram of the quadrotor coordinate systems is illustrated in Fig. 2, where $\mathbb{F}^I = \{x^I, y^I, z^I\}$ indicates an inertial coordinate system and $\mathbb{F}_i^B = \{x_i^B, y_i^B, z_i^B\}$ indicates a body-fixed coordinate system for the *i*th quadrotor. The set of swarm systems with N quadrotors can be described by $U = \{1, 2, \ldots, N\}$. Let $p_i(t) = [p_{xi}, p_{yi}, p_{zi}]^T$ and $v_i(t) = [v_{xi}, v_{yi}, v_{zi}]^T$ represent the position and velocity of the *i*th quadrotor in the inertial frame. $\mathbf{\Theta}_i(t) = [\phi_i, \theta_i, \psi_i]^T$ and $\mathbf{\Omega}_i(t) = [p_i, q_i, r_i]^T$ are denoted as Euler angles and angular rates of the *i*th quadrotor in the body frame. The six degrees of freedom (6DOF) mathematical model of the *i*th quadrotor is given by

$$\begin{cases} \dot{p}_i = v_i \\ m_i \dot{v}_\mathbf{i} = -m_i g \boldsymbol{\xi_3} + F_i R\left(\mathbf{\Theta_i}\right) \boldsymbol{\xi_3} \\ \dot{\mathbf{\Theta}}_i = \mathbf{\Xi}\left(\mathbf{\Theta}_i\right) \mathbf{\Omega}_i \\ J_i \dot{\mathbf{\Omega}}_i = -\mathbf{\Omega}_i \times J_i \mathbf{\Omega}_i + T_i \end{cases} \tag{1}$$

where g is the gravity constant, $J_i = diag(J_{xi}, J_{yi}, J_{zi})$ and m_i are the diagonal inertia matrix and the mass of the *i*th quadrotor, respectively, and $\boldsymbol{\xi}_3 = [0, 0, 1]^T$. $F_i \in \mathbb{R}^{1\times 1}$ and $T_i \in \mathbb{R}^{3\times 1}$ are the total lift and the control torque, respectively. Define an auxiliary control signal as $U_i^d(t) = -g\boldsymbol{\xi}_3 + \tilde{F}_i/m_i$ and $\tilde{F}_i = F_i R(\mathbf{\Theta_i})\boldsymbol{\xi}_3$. $R(\mathbf{\Theta}_i) \in SO(3) : \mathbb{F}^I \to \mathbb{F}_i^B$ is the orthogonal rotation matrix, which can be expressed as

$$R\left(\mathbf{\Theta}_i\right) = \begin{bmatrix} C_i^\theta C_i^\psi & S_i^\phi S_i^\theta C_i^\psi - C_i^\phi S_i^\psi & S_i^\phi S_i^\psi + C_i^\phi S_i^\theta C_i^\psi \\ C_i^\theta S_i^\psi & S_i^\phi S_i^\theta S_i^\psi + C_i^\phi C_i^\psi & C_i^\phi S_i^\theta S_i^\psi - S_i^\phi C_i^\psi \\ -S_i^\theta & S_i^\phi C_i^\theta & C_i^\phi C_i^\theta \end{bmatrix} \tag{2}$$

And the attitude kinematic matrix $\mathbf{\Xi}(\mathbf{\Theta}_i)$ is described as

$$\mathbf{\Xi}\left(\mathbf{\Theta}_i\right) = \begin{bmatrix} 1 & S_i^\phi T_i^\theta & C_i^\phi T_i^\theta \\ 0 & C_i^\phi & -S_i^\phi \\ 0 & S_i^\phi \left(C_i^\theta\right)^{-1} & C_i^\phi \left(C_i^\theta\right)^{-1} \end{bmatrix} \tag{3}$$

where C, S, and T are the abbreviations of $\cos(\cdot)$, $\sin(\cdot)$ and $\tan(\cdot)$, respectively.

In terms of research status and development trend of cooperative control for multiple quadrotors, dynamic formation is conducive to multiple quadrotors to complete complex tasks. In addition, in a complex environment, it is very important to avoid external obstacles and collisions between quadrotors. Therefore, the cooperative control problem is separated into the following two subproblems.

Problem 1 (Formation Tracking Problem): It is necessary to design a formation tracking protocol so that each quadrotor can quickly form the desired fixed or dynamic formation.

Problem 2 (Collision Avoidance and Obstacle Avoidance Problem): Firstly, a collision avoidance strategy is designed to make the minimum distance between quadrotors greater than the safety threshold. Secondly, an obstacle avoidance control strategy is designed to enable the quadrotors to avoid static or dynamic obstacles in an orderly and timely manner.

III. Methodology

In this section, firstly, a formation tracking protocol is proposed based on the consensus theory, which enables multiple quadrotors to quickly achieve a fixed or time-varying formation. However, the formation tracking protocol cannot ensure collision avoidance between quadrotors and external obstacles avoidance. Therefore, a novel collision avoidance mechanism and a novel obstacle avoidance mechanism are designed for quadrotors, and they are introduced into the formation tracking protocol to ensure that quadrotors do not collide while avoiding static or dynamic obstacles.

A. Formation Tracking Protocol

Let $s_i(t) = [p_i^T(t), v_i^T(t)]^T (i \in U)$ denote the state vector of the translational subsystem for the *i*th quadrotor and define the desired formation for multiple quadrotors to form by $c(t) = [c_1^T(t), c_2^T(t), \ldots, c_N^T(t)]^T \in \mathbb{R}^{6N\times 1}$ with piecewise continuously differentiable vector $c_i(t) = [pc_i^T(t), vc_i^T(t)]^T (i \in U)$, where $pc_i(t)$ and $vc_i(t)$ are the desired position and velocity vectors for the *i*th quadrotor.

Definition 1: Multiple quadrotors can achieve desired formation tracking, if and only if there is a vector $\boldsymbol{\delta}(t) \in \mathbb{R}^{6N\times 1}$ such that $\lim_{t\to\infty}(s_i(t) - c_i(t) - \boldsymbol{\delta}(t)) = 0 (i \in U)$, where $\boldsymbol{\delta}(t)$ is called a formation center function.

Therefore, based on consensus theory and the state information between quadrotors, the following distributed formation tracking protocol is designed for the *i*th quadrotor

$$u_i^f = K_1^f (s_i - c_i) + K_2^f \sum_{j\in U} w_{ij} [(s_j - c_j) - (s_i - c_i)] + vc_i \tag{4}$$

where $K_1^f \in \mathbb{R}^{3\times 6}$ and $K_2^f \in \mathbb{R}^{3\times 6}$ are feedback matrices, K_1^f is used to drive the movement of the formation center, and K_2^f is used to control quadrotors to achieve the desired formation. w_{ij} is the communication weight. $w_{ij} = 1$ if and only if q_j is the neighbor of q_i, else $w_{ij} = 0$. vc_i is the differential of the desired velocity vc.

Remark 1: It is worth noting that the formation tracking protocol adopted is a general formation protocol based on the consensus theory. When $c_i(t) = 0$, reaching agreement on certain variables is equivalent to realizing the desired formation for multiple quadrotors. The simple consensus problem is a special case of the formation tracking control problem.

Remark 2: It should be noted that the formation tracking protocol designed can enable multiple quadrotors to quickly achieve the desired fixed formation or dynamic formation, but it cannot guarantee the collision avoidance between quadrotors. Secondly, it is impossible to avoid static obstacles or dynamic obstacles.

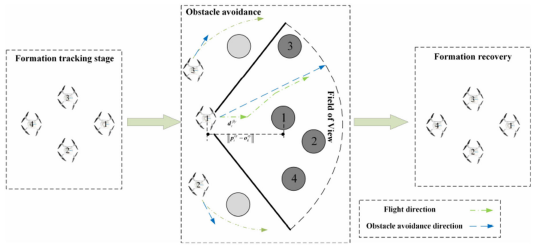

Fig. 3. Split-merge strategy of the quadrotors.

B. Collision Avoidance

When multiple quadrotors converge to the desired formation, the distance between quadrotors should not be less than the safe distance. To ensure quadrotor flight safety, it is very important to design the collision avoidance mechanism between quadrotors. To avoid collisions between multiple quadrotors in a timely and effective manner, it is not enough to consider only the relative position of multiple quadrotors, but also the relative velocity between quadrotors. In this work, a repulsion function based on Hooke's law with damping is added to the formation control protocol. Repulsion keeps the *i*th quadrotor away from other quadrotors only if the distances between them are less than the safety threshold. The repulsion function for the *i*th quadrotor is designed as follows

$$\begin{cases} u_{ij}^c = k_1^c p_{ji}^c + k_2^c v_{ij}^{xy} \\ p_{ji}^c = (R_c - ||p_{ij}^{xy}||)\dfrac{p_{ji}^{xy}}{||p_{ji}^{xy}||} \end{cases} \tag{5}$$

where k_1^c and k_2^c are the gain, R_c is the threshold to trigger collision avoidance for quadrotors and $p_{ji}^{xy} = p_j^{xy} - p_i^{xy}$.

Remark 3: The real-time kinematic (RTK) positioning system is adopted in the multiple quadrotors experimental platform, and the communication between quadrotors is carried out by wireless local area networks (WLANs). According to the designed communication topology, the *i*th quadrotor can obtain the position and velocity information of its neighbors to determine whether the collision avoidance should be triggered.

C. Obstacle Avoidance

In a complex environment, ensuring the safe flight of multiple quadrotors is also an important research topic. Inspired by the flight behavior of pigeons crossing narrow spaces, a split-merge strategy is adopted to design the steering controller for multiple quadrotors to avoid static and dynamic obstacles. The steering controller is driven by the relative position between the quadrotors and the obstacles. The split-merge mechanism of the multiple quadrotors is shown in Fig. 3.

1) Obstacle Detection: The pigeon's visual perception is sector-shaped, which is mapped to multiple quadrotors to give the following definition. The vertex of the perception region is defined as (p_{xi}, p_{yi}), the radius is R_p, and the perception region falls within $\pm\theta_p$ of the flight direction d_i^{fly}, where

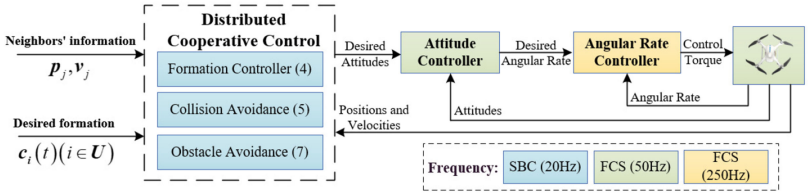

Fig. 4. A cascade control scheme for multiple quadrotors. The distributed cooperative controller runs at 20 Hz on the SBC. The attitude controller and angular rate controller run at 50 Hz and 250 Hz on the FCS, respectively.

$\theta_p \in (0, 2\pi)$ and $R_p > 0$. The set of obstacles is defined as $o = \{o_1, o_2, \ldots, o_t\}$, where t is the number of obstacles. $o_k = \{o_{xk}, o_{yk}, o_{zk}, o_{rk}\}^T$ is the *k*th position information of the obstacle, where (o_{xk}, o_{yk}, o_{zk}) is the center of the *k*th obstacle and o_{rk} is the radius of the *k*th obstacle. When the *i*th quadrotor detects the *k*th obstacle, it must meet the following two conditions

$$\begin{cases} ||p_i^{xy} - o_k^{xy}|| \leq R_p \\ |atan\dfrac{o_{yk} - p_{yi}}{o_{xk} - p_{xi}} - d_i^{fly}| \leq \theta_p \end{cases} \tag{6}$$

where p_i^{xy} and o_k^{xy} are the horizontal positions of the *i*th quadrotor and the *k*th obstacle, respectively. The above conditions are that if the distance between the *i*th quadrotor and the *k*th obstacle is less than or equal to R_p and the angle between the flight direction of the quadrotor and the obstacle is less than or equal to θ_p, then the quadrotor detects the obstacle.

2) Steering Implementation: Pigeons adjust their current flight direction in real-time after detecting obstacles. When there are multiple obstacles in the field of vision of the *i*th quadrotor, the position relationship between each obstacle and the *i*th quadrotor should be considered comprehensively. Then the optimal steering velocity is obtained to enable the quadrotor to fly to the maximum clearance between obstacles. The *i*th quadrotor's steering controller is designed as follows

$$u_{ik}^o = k_1^{obs} p_{ik}^{obs} + k_2^{obs} v_i \tag{7}$$

where k_1^{obs} and k_2^{obs} are constant gains. p_{ik}^{obs} is the position effect vector between the quadrotor and the obstacle, which is expressed as follows

$$p_{ik}^{obs} = sign(p_i)(o_k - p_i - R_o) f_{ik}^{dir} \tag{8}$$

$$\begin{cases} f_{x,ik}^{dir} = sign(po_{x,ik}) k_x^v (R_o - po_{x,ik}) \\ f_{y,ik}^{dir} = sign(po_{y,ik}) k_y^v (R_o - po_{y,ik}) \end{cases} \tag{9}$$

where R_o is the threshold to trigger obstacle avoidance, f_{ik}^{dir} is used to control the steering of the *i*th quadrotor, $po_{x,ik} = |p_{xi}| - |o_{xk}|$. k_x^v and k_y^v are the strengths of the steering velocity. In the experiment, the quadrotors fly in the negative direction of the Y-axis, so $k_y^v < 0$, and the flight direction is along the Y-axis, so $f_{y,ik}^{dir}$ can be simplified as $f_{y,ik}^{dir} = sign(po_{y,ik}) k_y^v$.

From (4), (5) and (7), the formation controller with collision avoidance and obstacle avoidance is obtained as follows

$$U_i^d = k_1^d u_i^f - k_2^d \sum_{j=1}^{N} u_{ij}^c - k_3^d \sum_{k=1}^{t} u_{ik}^o \tag{10}$$

where k_1^d, k_2^d and k_3^d are the strengths of the three control strategies. Therefore, k_2^d and k_3^d can be appropriately increased to ensure the safety of multiple quadrotors. $U_i^d(t) = [u_{xi}^d, u_{yi}^d, u_{zi}^d]^T$ is the expected acceleration of the *i*th quadrotor. The control strategy is shown in Fig. 4.

Remark 4: It is assumed that each quadrotor is equipped with optical sensors (e.g., lidar, binocular vision) that can detect obstacles and obtain their position information. It should be noted that this assumption is only used to avoid obstacles.

From (1), the model of a quadrotor is divided into a translational subsystem and a rotation subsystem. The above control protocol $U_i^d(t)$ is for the translational subsystem, and then the control command of the rotation subsystem needs to be solved. Considering $U_i^d(t) = -g\boldsymbol{\xi}_3 + \tilde{F}_i/m_i$ and the desired command of the rotation subsystem can be solved by the following equation.

$$\begin{cases} \theta_i^d = atan\dfrac{u_{xi}^d C_i^\psi + u_{yi}^d S_i^\psi}{u_{zi}^d + g} \\ \phi_i^d = asin\dfrac{u_{xi}^d S_i^\psi - u_{yi}^d C_i^\psi}{\sqrt{(u_{xi}^d)^2 + (u_{yi}^d)^2 + (u_{zi}^d + g)^2}} \\ \psi_i^d = \psi_i^0 \end{cases} \tag{11}$$

where ψ_i^0 is the initial yaw angle of the *i*th quadrotor.

After obtaining the desired attitude angle, it is necessary to design an appropriate attitude controller. Many scholars have studied the design of attitude controller for quadrotors (see e.g., [25], [26]). This work focuses on the design of the control protocol of the translational subsystem of multiple quadrotors, so for the convenience of the actual flight, a double closed-loop PID (Proportion Integral Differential) control is adopted in the rotation subsystem.

IV. Simulation Results and Experimental Results

In this section, the components of the multiple quadrotors experimental platform are firstly introduced, and then the effectiveness of the above theoretical results is verified by the simulation results and experimental results.

A. Multiple Quadrotors Platform

The components of the multiple quadrotors platform are presented in Fig. 5. The quadrotors are provided by EFY Intelligent Control (Tianjin) Technology Co., Ltd. Each quadrotor is mainly composed of a flight control system (FCS), a single board computer (SBC), a positioning module and a communication module. The wheelbase, weight and maximum flight time of

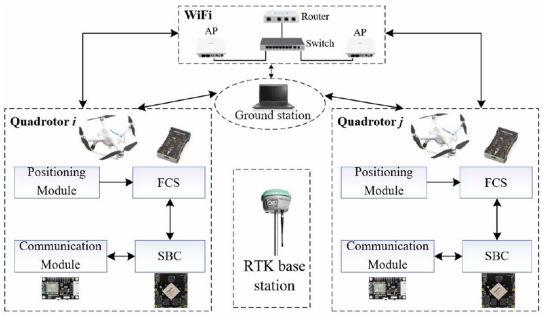

Fig. 5. Hardware structure of the multiple quadrotors platform.

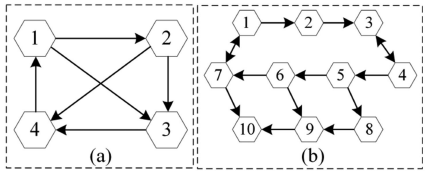

Fig. 6. Communication topology of the multiple quadrotors.

each quadrotor are 350 mm, 1450 g and 30 min, respectively. Each quadrotor is equipped with an RTK positioning module and a dual redundant internal measurement unit module (IMU) sensor. Multiple quadrotors communicate with each other via wireless local area networks (WLANs), which are composed of wireless access points (APs), a router and a switch. It should be noted that all the algorithms are run on the SBC and the FCS. The ground station only monitors the quadrotors' states without sending commands. Next, we carried out several experiments and recommended watching the videos to obtain a clearer understanding of the experimental scenarios and results. It can be found at: https://youtu.be/eseBaaZY6pc.

B. Obstacle Avoidance Results of Static Obstacles

1) Experiment With Two Quadrotors: In this scenario, two quadrotors are used as static obstacles. The center of the obstacle is the current coordinate of the quadrotor, and the radius of the obstacle is 2 m. The distance between the two obstacles is 4 m. The maximum velocity and acceleration of each quadrotor are $v_{max} = 2\ m/s$ and $a_{max} = 5\ m/s^2$. Additionally, the parameters of collision avoidance are chosen as $R_c = 1.8\ m$, $k_1^c = 40$, and $k_2^c = 2$. The parameters of obstacle avoidance are $R_p = 5\ m$, $\theta_p = 0.3\pi$, $k_1^{obs} = 10$, $k_2^{obs} = 0.5$, $k_x^v = 0.15$ and $k_y^v = -0.1$. The weights of the three control strategies are $k_1^d = k_3^d = 1$ and $k_2^d = 2$.

Fig. 7 shows the position trajectories of the four quadrotors in the experiment, where the initial positions of the quadrotors and obstacle are marked by diamonds and pentagrams, respectively. The figure on the upper left shows the outdoor flight results. It can be seen that two quadrotors can safely avoid obstacles without collision.

2) Experiment With Four Quadrotors: In this scenario, multiple quadrotors first form the desired formation based on the formation tracking protocol, and then cross the obstacles area. The communication topology of multiple quadrotors is presented

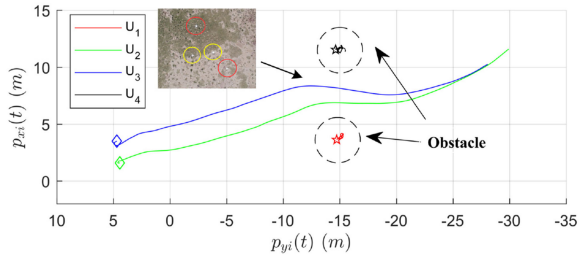

Fig. 7. Obstacle avoidance trajectory of two quadrotors in the experiment.

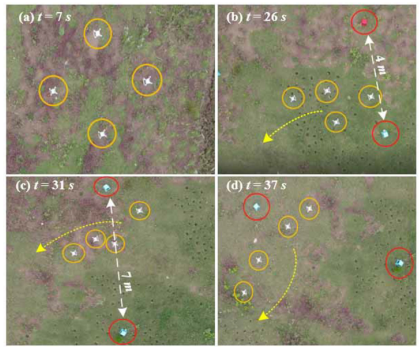

Fig. 8. Avoiding static obstacles for two quadrotors in the experiment.

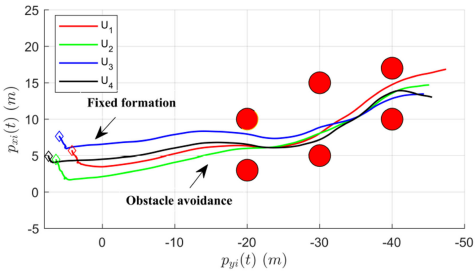

Fig. 9. Obstacle avoidance trajectories of four quadrotors in the experiment.

in Fig. 6(a). In the experiments, all quadrotors move on the horizontal plane. Consider the formation $c_i(t)$ with $pc_{xi}(t) = \beta + \alpha\cos(2\pi(-i)/4)$, $pc_{yi} = \alpha\sin(2\pi(-i)/4)$ and $vc_i(t) = 0_{3\times1}$ $(i = 1, 2, 3, 4)$. Choose $\beta = 5\ m$, $\alpha = 5/\sqrt{2}\ m$, $K_1^f = I_3 \otimes [-2.5, -2.8]$ and $K_2^f = I_3 \otimes [1, 1.2]$. Therefore, the desired formation shape of the multiple quadrotors is a square with edge 2.5 m. $k_x^v = 0.15$ and $k_y^v = -0.05$ and other parameters are consistent with the above experiment.

Fig. 8 displays the flight path of four quadrotors in the experiment. Figs. 9 and 10 display the position and velocity trajectories of the four quadrotors in the experiment, where the initial positions of the quadrotors are marked by diamonds. It can be seen that four quadrotors can form the desired formation, and they can effectively avoid obstacles in an environment with a minimum obstacle spacing of 4 m. It also clearly shows that quadrotors do not collide during the flight.

3) Simulation With Ten Quadrotors: The directional communication topology of ten quadrotors is shown in Fig. 6(b). The given formation is triangular and the distance between the

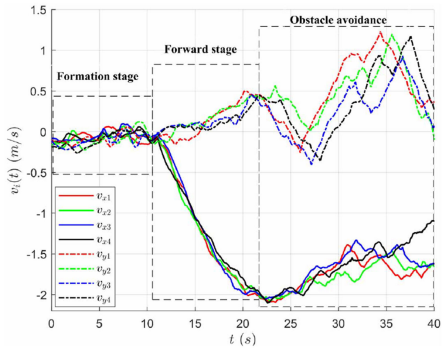

Fig. 10. Velocity trajectories of four quadrotors in the experiment.

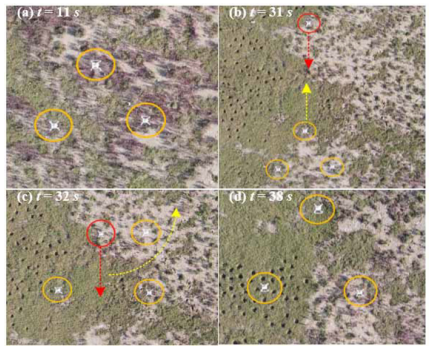

Fig. 12. Avoiding dynamic obstacles for quadrotors with fixed formation.

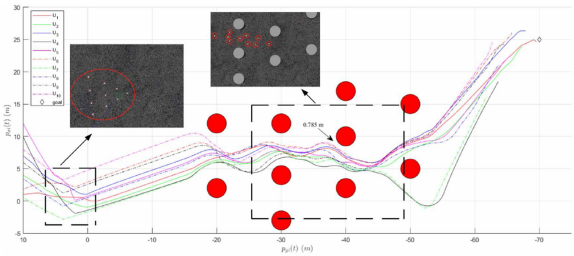

Fig. 11. Obstacle avoidance trajectories of ten quadrotors in Gazebo.

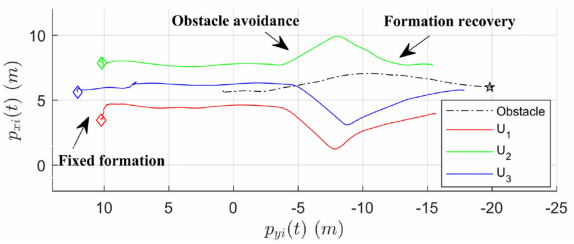

Fig. 13. Position trajectories of quadrotors with fixed formation.

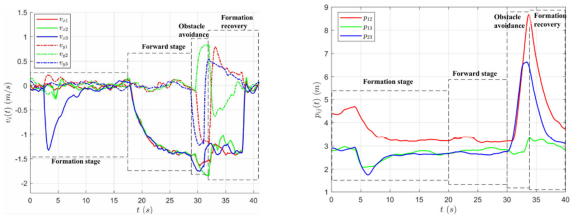

(a) Velocity trajectories. (b) Distance with other quadrotors.

Fig. 14. Flight status of quadrotors with fixed formation.

two adjacent quadrotors is 2 m. $k_x^v = 1.2$, $k_y^v = -2.2$, $k_2^d = 2$ and other parameters stay the same. The simulation results of ten quadrotors crossing ten obstacles are as follows. Fig. 11 displays the flight path of ten quadrotors in the Gazebo robotic simulator. The minimum distance between obstacles is 5 m, the minimum distance between ten quadrotors and obstacles is 0.785 m generated by the quadrotor q_{10}, and the minimum distance between quadrotors is 0.690 m generated by quadrotor q_4 and quadrotor q_5.

C. Obstacle Avoidance Results of Dynamic Obstacles

In this scenario, one quadrotor is used as a dynamic obstacle, while the other three quadrotors maintain static formation and dynamic formation to avoid moving obstacle. The velocity of moving obstacles is 1 m/s.

1) Experiment With Fixed Formation: The given static formation is a triangle. $k_x^v = 0.65$, $k_y^v = -1.5$ and other parameters are consistent with the scenario of four quadrotor. The forward velocity of the quadrotors is -1 m/s. Fig. 12 shows the flight of three quadrotors in formation, obstacle avoidance, and formation recovery. Figs. 13 and 14(a) show the position and velocity trajectories of quadrotors in the formation tracking stage, forward stage, obstacle avoidance stage and formation recovery for the experiment with fixed formation, where the initial positions of the quadrotors and obstacle are marked by diamonds and pentagrams, respectively. The distance between the quadrotors is shown in Fig. 14(b). From Figs. 12 to 14, one can see that three quadrotors can achieve the triangle formation, and collisions between the quadrotors are also avoided while avoiding the moving obstacle. From Fig. 14(b), it takes less than 5 s for multiple quadrotors from the end of obstacle avoidance to formation recovery.

2) Experiment With Dynamic Formation: The given dynamic formation $c_i(t)(i \in 1, 2, 3)$ with $pc_{xi} = \alpha\cos(\gamma t + 2\pi(i-1)/3)$, $pc_{yi} = \alpha\sin(\gamma t + 2\pi(i-1)/3)$, $vc_{xi} = -\gamma\alpha\sin(\gamma t + 2\pi(i-1)/3)$ and $vc_{yi} = \gamma\alpha\cos(\gamma t + 2\pi(i-1)/3)$, where $\alpha = 3\ m$ and $\gamma = 0.05\ rad/s$. $k_x^v = 0.65$, $k_y^v = -1.5$ and other parameters are consistent with the scenario of four quadrotors avoiding obstacles. The forward X-axis velocity and Y-axis velocity of the quadrotors are $0.4\ m/s$ and $-0.4\ m/s$, respectively.

Fig. 15 illustrates the formation producing, obstacle avoidance process and formation recovery in the flight experiment. Figs. 16 and 17(a) show the position and velocity trajectories of multiple quadrotors in the formation tracking stage, forward stage, obstacle avoidance stage and restore formation for the experiment with dynamic formation, where the initial positions of the quadrotors and obstacle are marked by diamonds and pentagrams, respectively.

The distance between the quadrotors is shown in Fig. 17(b). Figs. 15 to 17 show that three quadrotors can achieve the given

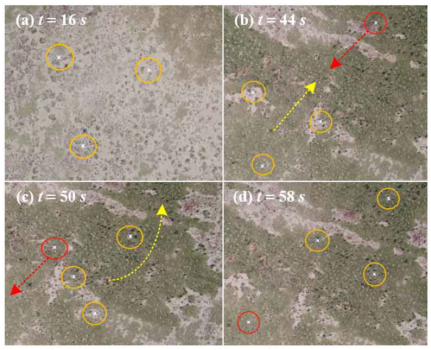

Fig. 15. Avoiding dynamic obstacles for quadrotors with dynamic formation.

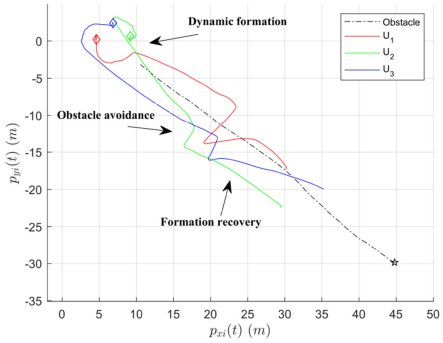

Fig. 16. Position trajectories of quadrotors with dynamic formation.

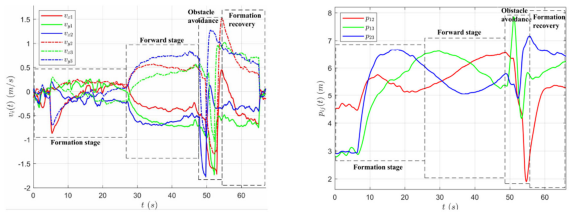

(a) Velocity trajectories. (b) Distance with other quadrotors.

Fig. 17. Flight status of quadrotors with dynamic formation.

circular dynamic formation and avoid obstacles in time. And it can be seen from Fig. 17(b) that it takes less than 4 s for multiple quadrotors from the end of obstacle avoidance to formation recovery.

D. Parameter Analysis and Algorithm Comparison

The key parameters of the designed obstacle avoidance mechanism are the strengths of the steering velocity k_x^v and k_y^v, which determine the trend of obstacle avoidance for multiple quadrotors. To better illustrate the robustness of the designed obstacle avoidance algorithm, several groups of experiments are carried out in the Gazebo robotic simulator to illustrate the influence of choosing different k_x^v and k_y^v on the experiment by taking multiple quadrotors crossing dense obstacle areas as an example. In actual flight, multiple UAVs fly to the south, so $k_y^v < 0$. Consider the following three cases: (1) $k_x^v > \mid k_y^v \mid$; (2) $k_x^v = \mid k_y^v \mid$; (3) $k_x^v < \mid k_y^v \mid$.

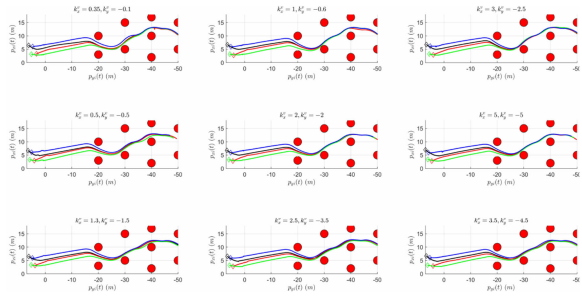

Fig. 18. Position trajectories under different obstacle avoidance parameters.

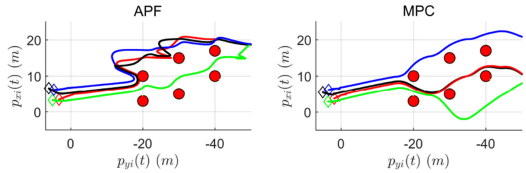

Fig. 19. Obstacle avoidance results of static obstacles.

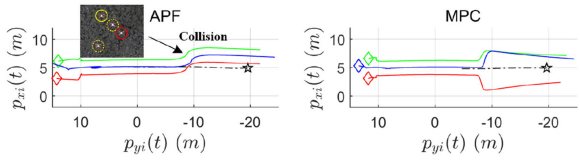

Fig. 20. Position trajectories under different obstacle avoidance parameters.

It can be seen from Fig. 18 that the size of the strengths of the steering velocity k_x^v, k_y^v has little effect on the experimental results. Under different parameters, multiple quadrotors can still avoid external obstacles well. The larger the $\mid k_y^v \mid$ is, the more unfavorable it is to adjust the formation of multiple quadrotors. When $k_x^v > \mid k_y^v \mid$, the effect of multiple quadrotors to avoid static obstacles is the best. The larger k_x^v allows multiple quadrotors to avoid obstacles in time, and the smaller $\mid k_y^v \mid$ allows multiple quadrotors to flexibly adjust their formation. When crossing narrow areas, multiple quadrotors are not suitable for avoiding obstacles with fixed squares or triangles. Multiple quadrotors need to adjust the formation in time to successfully cross dense obstacle areas. When avoiding dynamic obstacles, selecting $\mid k_y^v \mid$ greater than k_x^v can make multiple quadrotors better maintain the desired formation and facilitate the rapid convergence of formation.

Furthermore, a comparison with two state-of-the-art approaches, modified APF [17] and MPC [20] is given. Fig. 19 shows that APF cannot solve the problem of multiple quadrotors crossing dense obstacles well, and the trajectory generated by it is not smooth. MPC can solve the obstacle avoidance problem well, but it cannot guarantee the consistency of multiple quadrotors. Figs. 20 and 21 show that the obstacle avoidance effect produced by APF has a slow response and cannot avoid dynamic obstacles in time, where the quadrotors marked by dotted lines collide with dynamic obstacles. Although MPC can avoid dynamic obstacles in time, formation convergence takes a long time.

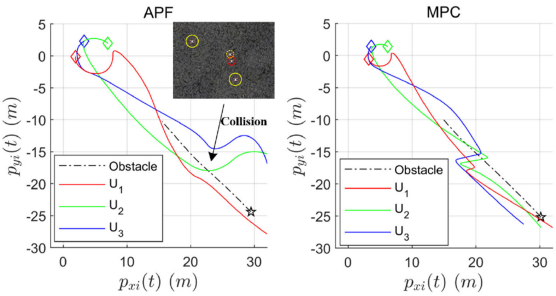

Fig. 21. Position trajectories under different obstacle avoidance parameters.

V. Conclusion

In this work, a distributed cooperative control algorithm for multiple quadrotors was developed to handle the problem of collision avoidance and obstacle avoidance during formation tracking. The collision avoidance strategy considered the relative velocity between quadrotors, which can avoid the collision of multiple quadrotors in time. A pigeon steering controller was designed to solve the problem of avoiding static and dynamic obstacles for multiple quadrotors. This method has lower complexity and can greatly reduce the calculation burden of quadrotors. Several outdoor experiments were conducted to verify the effectiveness of the method. The results show that multiple quadrotors could cross the obstacle area with a horizontal spacing of 4 m without collision and ensure the consistency of multi-quadrotors formation. Moreover, the time from the completion of multiple quadrotors avoiding dynamic obstacle to formation recovery is less than 5 s.

Increasing the number of quadrotors and the time delay problem in distributed cooperative control is a future research direction. Additionally, another future research is to consider the cooperative control and autonomous planning of multiple quadrotors in the denied environment.

References

[1] M. Gheisari and B. Esmaeili, "Applications and requirements of unmanned aerial systems (UASs) for construction safety," *Saf. Sci.*, vol. 118, pp. 230–240, 2019.

[2] M. Petrlik, T. Baca, D. Hert, M. Vrba, and M. Saska, "A robust UAV system for operations in a constrained environment," *IEEE Robot. Autom. Lett.*, vol. 5, no. 2, pp. 2169–2176, Apr. 2020.

[3] T. I. Zohdi, "Multiple UAVs for mapping: A review of basic modeling, simulation, and applications," *Annu. Rev. Environ. Resour.*, vol. 43, pp. 523–543, 2018.

[4] M. Coppola, K. N. Mcguire, C. D. Wagter, and G. Croon, "A survey on swarming with micro air vehicles: Fundamental challenges and constraints," *Front. Robot. AI*, vol. 7, pp. 1–26, 2020.

[5] S. Huang, R. S. H. Teo, and K. K. Tan, "Collision avoidance of multi unmanned aerial vehicles: A review," *Annu. Rev. Control*, vol. 48, pp. 147–164, 2019.

[6] G. Vásárhelyi, C. Virágh, G. Somorjai, T. Nepusz, A. E. Eiben, and T. Vicsek, "Optimized flocking of autonomous drones in confined environments," *Sci. Robot.*, vol. 3, no. 20, pp. 1–13, 2018.

[7] H. Yang, L. Cheng, and J. Zhang, "Leader-follower trajectory control for quadrotors via tracking differentiators and disturbance observers," *IEEE Trans. Syst., Man, Cybern.: Syst.*, vol. 51, no. 1, pp. 601–609, Jan. 2021.

[8] I. Bayezit and B. Fidan, "Distributed cohesive motion control of flight vehicle formations," *IEEE Trans. Ind. Electron.*, vol. 60, no. 12, pp. 5763–5772, Dec. 2013.

[9] Y. Abbasi, S. A. A. Moosavian, and A. B. Novinzadeh, "Formation control of aerial robots using virtual structure and new fuzzy-based self-tuning synchronization," *Trans. Inst. Meas. Control*, vol. 39, no. 12, pp. 1906–1919, 2017.

[10] Y. Cao, W. Yu, W. Ren, and G. Chen, "An overview of recent progress in the study of distributed multi-agent coordination," *IEEE Trans. Ind. Inform.*, vol. 9, no. 1, pp. 427–438, Feb. 2013.

[11] L. Ding, Q. L. Han, X. Ge, and X. M. Zhang, "An overview of recent advances in event-triggered consensus of multiagent systems," *IEEE Trans. Cybern.*, vol. 48, no. 4, pp. 1110–1123, Apr. 2018.

[12] W. Ren, "Consensus strategies for cooperative control of vehicle formations," *IET Control Theory Appl.*, vol. 1, no. 2, pp. 505–512, 2007.

[13] H. Liu, T. Ma, F. L. Lewis, and Y. Wan, "Robust formation control for multiple quadrotors with nonlinearities and disturbances," *IEEE Trans. Cybern.*, vol. 50, no. 4, pp. 1362–1371, Apr. 2020.

[14] X. Dong, Z. Yan, R. Zhang, and Y. Zhong, "Time-varying formation tracking for second-order multi-agent systems subjected to switching topologies with application to quadrotor formation flying," *IEEE Trans. Ind. Electron.*, vol. 64, no. 6, pp. 5014–5024, Jun. 2017.

[15] X. Dong, Y. Hua, Y. Zhou, Z. Ren, and Y. Zhong, "Theory and experiment on formation-containment control of multiple multirotor unmanned aerial vehicle systems," *IEEE Trans. Autom. Sci. Eng.*, vol. 16, no. 1, pp. 229–240, Jan. 2019.

[16] S. A. Ajwad, E. Moulay, M. Defoort, T. Ménard, and P. Coirault, "Collision-free formation tracking of multi-agent systems under communication constraints," *IEEE Control Syst. Lett.*, vol. 5, no. 4, pp. 1345–1350, Oct. 2021.

[17] H. Heidari and M. Saska, "Collision-free trajectory planning of multi-rotor UAVs in a wind condition based on modified potential field," *Mech. Mach. Theory*, vol. 156, no. 1, pp. 1–16, 2021.

[18] J. Hu, M. Wang, C. Zhao, and Q. Pan, "Formation control and collision avoidance for multi-UAV systems based on Voronoi partition," *Sci. China Technol. Sci.*, vol. 63, no. 1, pp. 65–72, 2020.

[19] H. Guo, C. Shen, Z. H., and H. Chen, "Simultaneous trajectory planning and tracking using an MPC method for cyber-physical systems: A case study of obstacle avoidance for an intelligent vehicle," *IEEE Trans. Ind. Inform.*, vol. 14, no. 9, pp. 4273–4283, Sep. 2018.

[20] B. Lindqvist, S. S. Mansouri, A. A. Agha-Mohammadi, and G. Nikolakopoulos, "Nonlinear MPC for collision avoidance and control of UAVs with dynamic obstacles," *IEEE Robot. Autom. Lett.*, vol. 5, no. 4, pp. 6001–6008, Oct. 2020.

[21] C. Virágh *et al.*, "Flocking algorithm for autonomous flying robots," *Bioinspiration Biomimetics*, vol. 9, no. 2, pp. 1–11, 2014.

[22] P. Petráček, V. Walter, T. Báča, and M. Saska, "Bio-inspired compact swarms of unmanned aerial vehicles without communication and external localization," *Bioinspiration Biomimetics*, vol. 16, no. 2, pp. 1–19, 2020.

[23] H. T. Lin, I. G. Ros, and A. A. Biewener, "Through the eyes of a bird: Modelling visually guided obstacle flight," *J. Roy. Soc. Interface*, vol. 11, no. 96, pp. 1–12, 2014.

[24] M. Huo, H. Duan, Q. Yang, D. Zhang, and H. Qiu, "Live-fly experimentation for pigeon-inspired obstacle avoidance of quadrotor unmanned aerial vehicles," *Sci. China Inform. Sci.*, vol. 62, no. 5, pp. 1–8, 2019.

[25] F. Oliva-Palomo, A. J. Munoz-Vazquez, A. Sanchez-Orta, V. Parra-Vega, C. Izaguirre-Espinosa, and P. Castillo, "A fractional nonlinear pi-structure control for robust attitude tracking of quadrotors," *IEEE Trans. Aerosp. Electron. Syst.*, vol. 55, no. 6, pp. 2911–2920, Dec. 2019.

[26] B. Tian, J. Cui, H. Lu, L. Liu, and Q. Zong, "Attitude control of UAVs based on event-triggered supertwisting algorithm," *IEEE Trans. Ind. Inform.*, vol. 17, no. 2, pp. 1029–1038, Feb. 2021.